August 1972

LRP 54/72

CENTRE DE RECHERCHES EN PHYSIQUE DES PLASMAS

FINANCÉ PAR LE FONDS NATIONAL SUISSE DE LA RECHERCHE SCIENTIFIQUE

HIGH-POWER CO_2 TEA LASER STUDIES

P. Oettinger

LAUSANNE

August 1972 LRP 54/72

HIGH-POWER CO_2 TEA LASER STUDIES

P. Oettinger

A b s t r a c t

The need for a good interferometric and light scattering plasma diagnostic radiation source has resulted in a program to construct high-power, TEA, CO_2 lasers . A resistance-limited, 1.2-m long, pin-plate, plane-parallel oscillator, with a 4-cm electrode separation, has yielded maximum powers of 20 MW, energies approaching 2J,and electrical-to-radiation efficiencies near 9 % . Optimum CO_2:N_2:He gas composition was found to be 1.5:1.5:7 , operated at atmospheric pressure. Current pulse durations for the 60 kV discharges approximated 1 μs, with maximum amplitudes of 18 A per pin. Onset of lasing occurred near the end of the discharge with pulse half-widths of 60-150 ns. Increasing the electrode separation to 6 cm,doubling the capacitance of the system,and changing the gas composition to a 0.4-atmosphere 1:1:2 mixture, doubled the output energy. Concentric electrode configurations, using a wire cathode along the laser axis, surrounded by a cylindrical anode, lased at reduced powers, maximizing at 1.4 MW.

Lausanne

I. Introduction

A. Advantages of IR Diagnostics

The analyses of transient and energetic plasmas require sophisticated diagnostic techniques. Optical methods, which perturb the high-temperature gases the least, are evidently very desirable. When such diagnostics require external light sources, they are often optimized by the high power, coherent, and single wavelength properties of lasers. Specifically, precise interferometric and light scattering, spatial and temporal measurements of electron densities and particle temperatures rely heavily on the use of such strong laser sources. In particular, long wavelength systems offer distinct advantages, and have led to the use of the recently invented high-power, transversely excited atmospheric (TEA) CO_2 laser.

For example, the average electron density n_e along pathlength L, as can be determined from fringe shift S measurements[1],

$$n_e = -\frac{2\pi m c^2}{e^2}\,\frac{S}{\lambda_o L} \tag{1}$$

is seen to be inversely proportional to the light source wavelength λ_o. For toroidal plasma geometries, where short pathlength cross-sectional measurements are required, long wavelengths are imperative. Minimum densities of 10^{14} cm^{-3} can be observed at the CO_2 wavelength of 10.6 μ and a pathlength of 1.5 cm. The advent of infrared holography[2] has further extended the usefulness of IR interferometric analyses of transient plasmas[3,4].

A dominant consideration in scattering diagnostics is the amount of momentum transferred by the charged plasma particles to the incident photons.

A measure of this transfer is given by the following function[5]

$$\alpha = \frac{\lambda_o}{4\pi\lambda_D \sin\frac{\vartheta}{2}} \tag{2}$$

where ϑ is the scattering angle measured from the incident direction and λ_D is the plasma Debye length. When $\alpha > 2$ the momentum associated with the plasma oscillations is much greater than that transferred to the incident wave, thereby producing collective scattering effects in the plasma. It is evident from equation (2) that, for constant α, as λ_o increases so must ϑ, allowing such collective ion scattering to be viewed at angles sufficiently away from the difficult forward direction. For example, for a 40 eV plasma with an electron density of 10^{14} cm^{-3} a ruby laser (6943 Å) requires that $\vartheta < 0.7^\circ$, whereas a CO_2 laser (10.6μ) only demands that $\vartheta < 10.3^\circ$. Such increased viewing angles, as well as the longer wavelengths of IR lasers, result in better scattered line spectral measurements of the width of the central ion feature $\Delta\lambda$[5] from which ion temperatures T_i can be deduced, if electron temperatures T_e are known.

$$\Delta\lambda = 2\frac{\lambda_o}{c}\left(\frac{k(T_e + T_i)}{m_i}\right)^{1/2}\sin\frac{\vartheta}{2} \tag{3}$$

If the electron temperature is unknown it can be calculated from incoherent (Thomson) scattering measurements[6] which occur at viewing angles where $\alpha \leq 0.5$. Although IR lasers can in general be used in this domain, there are certain plasma conditions, notably high electron densities, where the use of long wavelengths is precluded. For example, no incoherent scattering domain exists for 10.6 μ radiation incident on a 40 eV plasma with $n_e \sim 10^{16}$ cm^{-3}.

Simultaneous T_e and n_e measurements can also be made by observing both the incoherently scattered profiles and their magnitudes[7]. Since absolute intensity determinations are difficult, a separate measurement of n_e can be made in the IR-accessible $0.5 < \alpha \leq 2$ regime by measuring the location $\Delta\lambda_s$, from the center of the scattered profile, of the shoulders formed in the modified Gaussian shape.

$$n_e\,[cm^{-3}] = 2.38\,(10^{13})\,(\Delta\lambda_s\,[\mathring{A}])^2 \tag{4}$$

This technique should provide a sensitive measurement, if the position of these shoulders can be adequately defined. Alternatively, if T_e is known, the position of the two detached satellites, at shifts $\Delta\lambda_t$ from the central ion feature in the readily IR-amenable collectively scattered domain, can be used to determine n_e

$$n_e\,[cm^{-3}] = 4.76\,(10^{13})(\Delta\lambda_t\,[\mathring{A}])^2 - 5.38\,(10^{-16})T_e\,[eV]\sin^2\frac{2\theta}{2} \tag{5}$$

Although the foregoing considerations show long wavelength lasers as advantageous over their visible wavelength counterparts for almost all plasma diagnoses, available infrared detection systems are only now becoming adequately sensitive to the short, weak signals emitted from transient plasmas. For exemple liquid He cooled Ge:Hg detectors are now manufactures with response times of less than 1 ns, and with $D^*_\lambda \sim 2\,(10^{10})$ cm $cps^{\frac{1}{2}}\,W^{-1}$. The noise equivalent power NEP_λ of such a 10 mm^2 detector at 10.6 μ for a pulse length $\tau \sim 100$ ns is

$$NEP_\lambda \sim \frac{1}{D^*_\lambda}\left(\frac{A}{\tau}\right)^{1/2} \sim 10^{-7}\ W \tag{6}$$

Since maximum scattered energies recorded by such small detectors are probably of the order of 10^{-13} - 10^{-14} less than the incident radiation, the detector's thermal noise will be negligible in comparison to the scattered radiation from 10-100 MW CO_2 lasers.

B. Power Requirements for Diagnostics and Fusion

In diagnosing transient plasmas with IR lasers interferometric measurements, which are least demanding, will require only MW systems, whereas 10-100 MW lasers will allow good scattering analyses. Further increases in power may eventually lead to laser-produced fusion. CO_2 lasers can effectively heat plasmas with $n_e \sim 10^{17}$ - 10^{19} cm^{-3}, whereas ruby or neodymium-glass devices are relatively ineffective at $n_e < 10^{19}$ cm^{-3} (8). Non linear absorption in imploding pellets may occur for laser powers of 10^{12} - 10^{14} W cm^{-2} (8,9), and may lead to the threshold condition, where fusion output equals radiation energy input, for lasers energies of 10^5 - 10^6 joules. Such levels would probably be radiated by 1-10 TW lasing systems which would be significantly more powerful than those presently existing. However, the phenomenal rise in CO_2 power levels - from several mW a few years ago to GW at present (10) - suggest that such limits are not unattainable in the future. Consequently, the development of high power CO_2 lasers is desirable from diagnostic as well as potential "fusion producer" stand points, and has prompted this laboratory to begin such a program, the details of which are discussed in the following sections.

II. Basic Laser System

A. Laser Design

The construction of the initial laser, based on systems developed in Canada (11) and at Garching, is shown in Fig. 1. One hundred 1-mm diameter pointed pins

were mounted in separate holes spaced 1 cm apart in a 10-cm diameter evacuable plexiglass tube. Each of these pins was connected to a current limiting 16 W, 1 KΩ resistor. This arrangement comprised the cathode of the laser which could be adjusted up and down perpendicular to the tube axis. A similarly moveable 5-mm diameter rod formed the anode. Electrode gap spacing between the pins and the rod could, thereby, be varied from 2 to 6 cm.

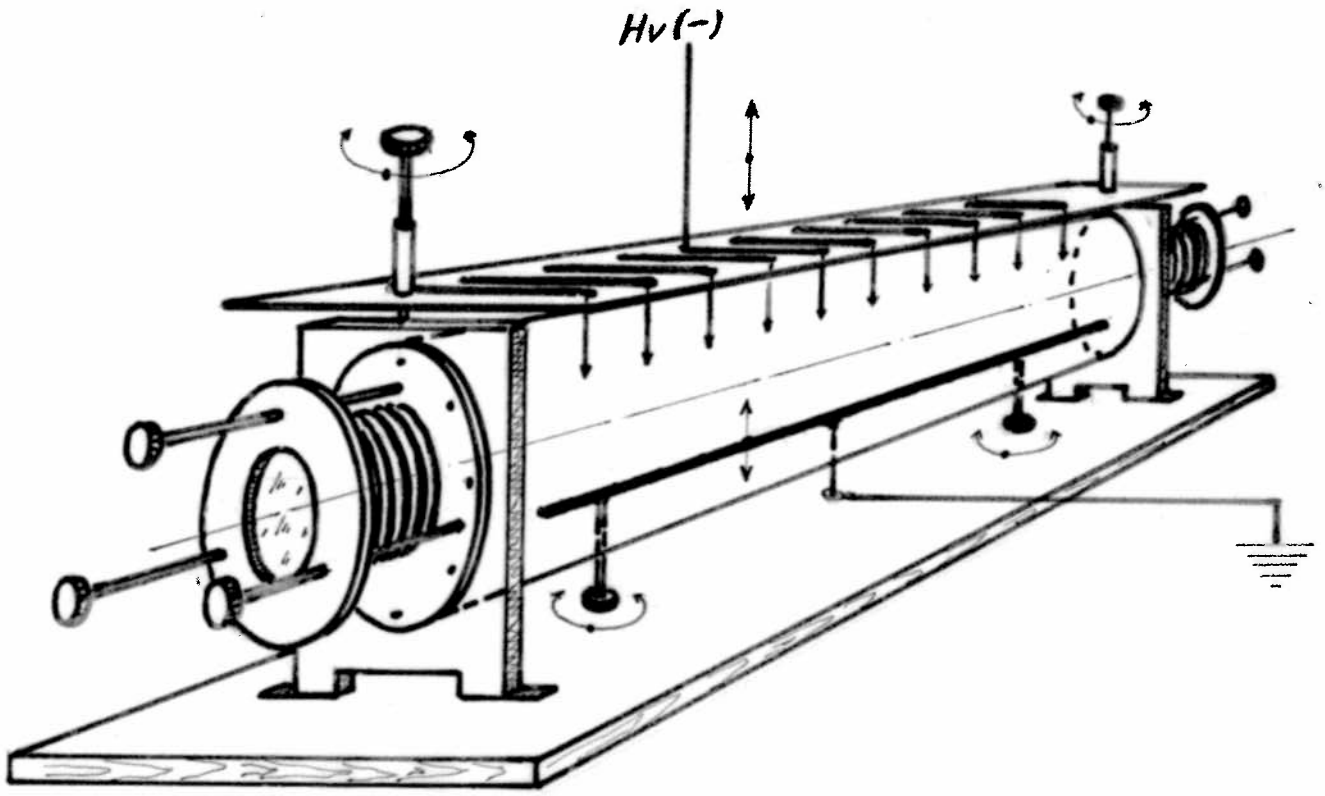

Fig. 1 Schematic Representation of Pin-Rod CO_2 laser

B. Optical Characteristics

The mirrors formed part of the evacuable cavity, being connected to the main tube by metallic bellows. Although mechanically less stable than a system using external mirrors, this arrangement removed the need of using Brewster angle windows to seal the cavity.

Initial rough mirror alignment was made with a standard He-Ne laser. Both partially transmitting (50 % and 65 % reflecting dielectric covered Germanium flats) and 4-mm diameter hole-coupled cavities were made to lase , with the former giving significantly higher powers. Full mirrors (plane and spherical) were made of glass ground to a flatness tolerance of 1/175 of the CO_2 wavelength and coated, via an evaporative process, with a layer of silver or gold. A protective coating of quartz (~ $\frac{1}{2}$ μ) covered several of the mirrors. Little difference was noted between the various coatings with respect to lasing effectiveness. Although the quartz seems to somewhat impede dust accumulation and scratching of the surfaces, cleaning of the mirrors was found almost impossible. However, visible amounts of dust and surface scratching did not seem to prevent lasing.

Various cavity configurations were studied. A carefully tuned, hemispherical resonator allowed the isolation of various lower order modes, from the "doughnut" $TEM_{01,10}$ up to what appeared to be the TEM_{04}. However, the spot size ω_s, i.e., $\frac{1}{2}$ the diameter of the Gaussian field distribution of the lowest order mode, on the output coupler of this cavity[12]

$$\omega_s = \left(\frac{\lambda_o}{\pi}\right)^{1/2} d^{1/4} (b-d)^{1/4} \qquad (7)$$

was so small (for a full mirror radius b minus mirror separation d of a few mm) to cause burning of the dielectric coating on the Ge flat. Though not excessively powerful, such a hemispherical cavity was, as expected, quite stable over long periods of experimentation, and the easiest to adjust.

Converting this configuration to a long-radius cavity with a fully reflecting mirror having a 5-m radius, i.e., approximately four times the mirror separation, increased the maximum output power threefold (as would be predicted from simple geometric considerations). Attempts at externally focussing the emitted beam to a small spot by a 1-m radius spherical mirror, proved unsuccessful, indicating some non-negligible divergence of the radiation. Several milliradian angular beam expansion ϕ is to be expected from higher order modes, whose lobe diameters ℓ are small[13].

$$\varphi \sim \frac{\lambda_o}{\ell} \tag{8}$$

However, conversion of the long-radius resonator to a plane-parallel cavity doubled the peak power and produced external small spot focussing, sufficient to cause pure, or possibly dust particle stimulated, air breakdown. Such effects indicated, from equ. (7,8), that the small-divergence lowest order mode most likely dominates in such a cavity. This conclusion was reinforced by noting that a spot was burned in the 5-m radius mirror corresponding to the size of the lowest order mode's Gaussian field, as well as from the absence of lasing in the hole-coupled confocal experiments, where the lowest order mode was "lost" through the hole.

C. Vacuum and Gas Handling Systems

A vacuum system composed only of a 1.4 ℓs^{-1} forepump allowed all pressure regimes to be investigated. For sub-atmospheric studies of the hole-coupled cavities a 170 μ layer of polyethylene, found to have a 72 % transmission at normal incidence of 10.6 μ radiation, covered the output hole. The essentials of this system are shown in Fig. 2. Both the filling and evacuation of the laser were done through the same port in the plexiglass tube. The gases were mixed inside the lasing cavity, by sequentially flowing in small amounts of each component, until the desired mixture and pressure was obtained.

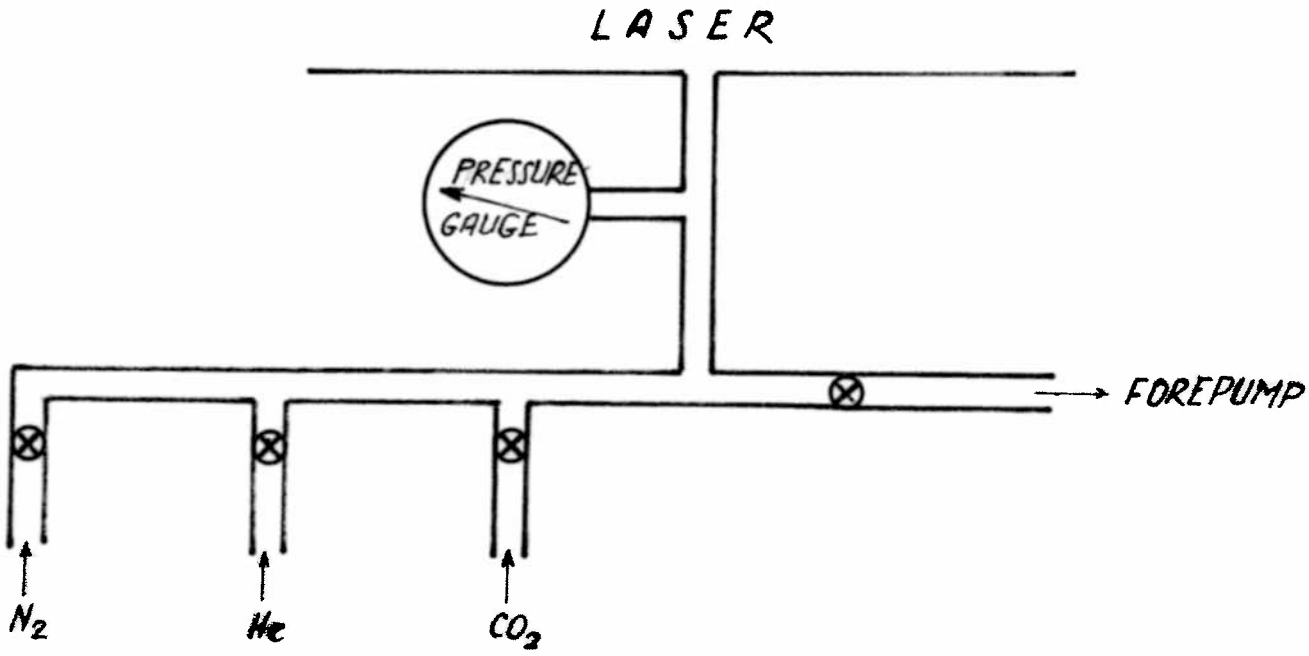

Fig. 2 Schematic of Gas Handling and Vacuum System

High grade gases were not found to be necessary since normal gas impurities were not observed to significantly degrade the lasing output.

D. Electrical Discharge Characteristics

Electrical power was initially supplied by a 12.5 nF, 30 kV, spark-gap triggered capacitor bank which was subsequently replaced by a voltage-doubling,two-stage Marx generator. Eventually the capacitance was raised to 24 nF. The design of this generator is shown in Fig. 3.

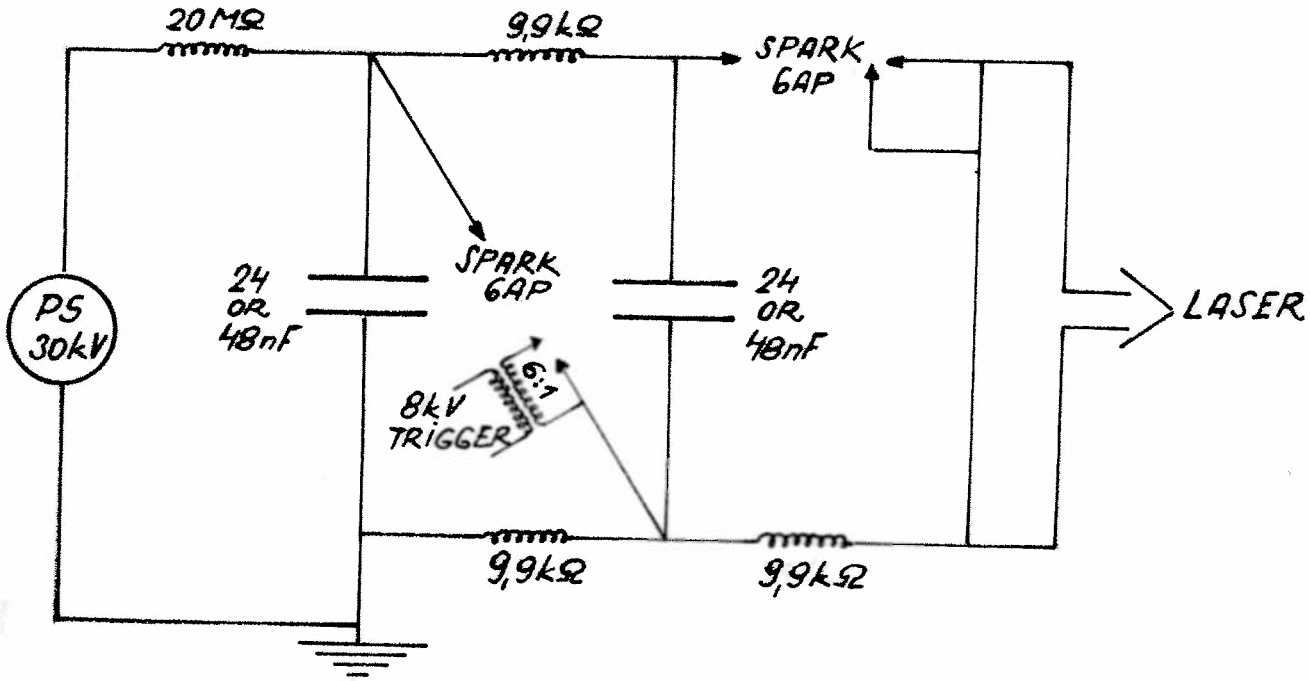

Fig. 3 Schematic of Two-Stage Marx Generator

An early parametric study indicated that for the 12.5 nF, 30 kV discharges maximum power is obtained at total gas pressures of approximately one-third atmospheres, with one-half to two-thirds of the mixture CO_2 and the rest N_2. Addition of He, rather than improve lasing, actually reduced power levels by raising the pressure excessively, and lengthened the delay time between the electrical discharge and the onset of radiation. An electrode spacing of 4 cm was found to optimize power levels, with a reduction to 2 cm decreasing the power approximately 30 %; while an increase to 6 cm resulted in a 70 % reduction. Maximum powers, recorded for the long-radius cavity, reached 1.5 MW with risetimes below 100 ns, halfwidths of 60-150 ns, and delays between the electrical discharge to the onset of radiation near

1 μs. Maximum discharge currents approximated 300 A with duration of the electrical discharge of about 2 μs.

During the second stage of experimentation the voltage-doubling, two-stage Marx generator, with nearly the same capacitance (12 nF) was used to increase maximum voltages to 60 kV; such voltage doubling having been observed in Canada[14] to increase peak radiative power levels by an order of magnitude. This generator appreciably increased the electronic noise near the experiment so that precise measurements of the electrical discharge characteristics required an oscilloscope shielded in a Faraday cage 20 m from the laser. Voltages, measured with a balanced R-C divider in conjunction with a 100 ns filter, indicated an inverse dependence of pulse-decay time with applied voltage. Pulse durations at the higher voltages were of the order of 1 μs. Negligible voltage losses occurred in the Marx circuit, as was verified by replacing the laser with a 200 Ω resistor, and recording the discharge voltage traces. Current measurements were made with an available calibrated probe[15], as well as with a simply-wound Rogowski coil. Deviations of less than 20 % were noted between these two devices. A steady increase in maximum current with increasing discharge voltage was noted, reaching 1900 A for 60 kV discharges in a CO_2:N_2:He - 1:1:0 gas mixture at 0.2 atmospheres. Addition of 0.8 atm He reduced the maximum current at this voltage by only 14 %. The total inductance of the system, made by short-circuiting the laser resistors and observing the resultant ringing frequency and decay time, was calculated to be about 100 nH. Calorimetric radiation energy measurements for a long-radius cavity indicated a linear dependence of total energy with discharge voltage from 0.194 J at 30 kV to 0.395 J at 60 kV (although these higher voltage values may be lower limits, as will be discussed further on).

Whereas at the lower voltages even small amounts of He increased the pressure sufficiently to cause strong arc formation due to excessive energy dissipation in the cathode-drop region[16] near the pins, as well as the long activation, or "jitter", time between pins, the addition of 8 parts of He

at 60 kV increased the IR output by 74 %. Visual observations suggest that these higher powers are due, at least in part, to a greater spreading of the discharges, thereby increasing the volume of excited gas. Consequently, further expansion of the discharge was attempted by clipping a 3-cm wide, 100-cm long plate onto the anode rod. The greater volume of excited gas, and consequently, the lowered current densities in the tube allowed a higher concentration of CO_2 in the mixture without the formation of strong arcs. Resulting power levels for the long-radius cavity, double over those achieved with the rod alone, reached 10 MW for a 60 kV discharge. Excellent shot-to-shot reproducibility of the radiation powers, profiles, and delays was noted at an atmospheric pressure CO_2:N_2:He - 1.5:1.5:7 gas mixture. A similar plane-parallel oscillator further doubled maximum powers to 20 MW, but proved less mechanically stable and reproducible.

As an interesting sidelight, small amounts of water vapor (1, 5, 10 and 15 Torr) were injected into the cavity in order to determine their effect on laser output. In contrast to previous studies[17], the vapor created strong arcing which prevented any significant lasing.

Although, a 4-cm electrode separation was found optimum for the laser system limited to 30 kV discharges, a 6-cm gap was found superior at 60 kV. In fact, for a doubling of the capacitance to 24 nF and a 0.4-atmosphere CO_2:N_2:He - 1:1:2 gas mixture (a combination which was found to limit the formation of arcs) calorimetric measurements indicated approximately twice the IR output as compared to the system with a 4-cm electrode separation and one-half the capacitance. Furthermore, for the 6-cm gap the laser beam was seen to be limited by the 4-cm diameter circular Germanium output aperature.

E. Detectors and Attenuators

Detection of the IR radiation was made with a screen of graphite powder sprinkled on tape to allow its use in a vertical position. A few drops of alcohol mixed with the graphite were found to produce a paste which could

be brushed uniformly over the tape. Strong 10.6 μ radiation (above 100 kW cm^{-2} [18]) burns the graphite, causing visible illumination with good spatial resolution, which is essential for recognizing mode patterns and making interferometric fringe measurements. Researchers at Garching have obtained resolutions of 0.1 mm [18] with such detectors. Similarly, Thermofax Type 11 paper was tested; Los Alamos having observed resolutions of 40 lines per mm [3]. Thermofax, however, has a higher activation threshold (approximately 2J cm^{-2} [3]) which is above the unfocussed output density of our laser. Focussed emission produced uniformly dark patterns.

Maximum radiation power levels and pulse profiles were measured with an Oriel Optik 7411 photon-drag detector having a sensitivity of 0.15 mV kW^{-1} and a response time of less than 1 ns. Traces were recorded in the Faraday cage 20 m from the experiment with the signal raised 20-fold by a fast response amplifier situated near the detector to reduce noise pick up in the long cables. The IR beam was focussed on the detector's 4-mm square Ge surface by a 1-m radius spherical mirror. A small, polished aluminium "light-funneling" cone was occasionally attached to the detector when focussed spot sizes exceeded the detector's area. Teflon sheets, each 1/4 mm thick, attenuated the beam in order to retain a linear response of the detector and prevent damage of its surface, as well as to prevent saturation of the amplifier (which occurred at input signals above 40 mV). Each such teflon sheet reduced the power level approximately 78 %. A stack of up to four such attenuators was used in high power experiments. The teflon sheets also allowed the linearity of the detector to be verified at power levels up to at least 1 MW focussed on its surface. At higher levels burning of the detector's face was noted, although the instrument continued to respond until the damage became excessive.

Radiated energies were measured with a conical thermocouple calorimeter originally designed and calibrated for Ruby laser diagnostics by P. Boulanger.

For the lower powers fair agreement was noted between the energies measured with this instrument and the integrated profiles observed with the photon-drag detector. However, at higher power levels there appeared to be significant discrepancies, the calorimeter reading consistently lower. Such differences might be attributed to air breakdown within the calorimeter's cone or on its surface, though this has as yet not been verified. Such calorimeter readings at least gave a lower bound of 1.5 J on the maximum energy.

Additional trials were made to determine the applicability of a "water" calorimeter, wherein the focussed beam would be absorbed by a thin layer of water. Such absorption is quite complete, since transmission through the water was not observed, and reflection at 10.6 μ is known to be less than 1 % at normal incidence[19]. However, approximately 4J are required to heat 1 gm of water $1^{o}C$, requiring this instrument to be used with lasers of considerably higher energies, or allowing low power measurements of only the mean energy of a number of pulses.

III. New Discharge Geometries

A. Concentric Mesh Laser

The amount of energy available from a gas laser is limited by the occurrence of photon induced electrical breakdown within the gas above a critical level of radiation density. Experiments have indicated that such breakdown may occur near $20J\ cm^{-2}$ [10]. Consequently, laser lengths will reach a limit, and it will be necessary to increase the effective area of the oscillator either by raising the diameter of a single unit, or by running a number of units in parallel and combining their outputs.

An attempt was made to increase the oscillator's diameter without requiring further increases in applied voltages by producing an axially symmetric discharge between a thin (0.3 mm) copper wire cathode strung along the axis of the laser and a 4-cm diameter, 100-cm long concentric copper wire mesh anode. In order to minimize the perturbation in the lasing volume due to such a wire, one could thread its ends through small holes in the mirrors. A simpler system, from a constructional point of view, uses a thin strut inside the cavity in front of each mirror to hold the wire and to connect it to the rest of the electrical circuit. The interference effects of such struts was measured in the pin-plate laser cavity to cause only minimal (less than 20 %) reductions in power levels. This concentric mesh configuration is shown in Fig. 4a. Optimum conditions for the cavity were found to result in maximum power levels of 1.4 MW for a plane parallel cavity filled with a one-half atmosphere CO_2:N_2:He - 1:1:3 gas mixture, for a capacitance of 12 nF, and a maximum discharge voltage of 60 kV. Because of the smaller electrode separation in this configuration, with respect to a comparable volume pin-plate system, the electric discharge times are somewhat shorter with larger maximum currents. In order to prevent arcing a 15 Ω resistor was required to be in series with the discharge. Increasing the energy by raising the capacitance resulted in arcing within the laser. A 10-cm diameter, 60-cm long configuration was also made to lase at reduced pressures. At higher pressures arcs were formed.

B. Concentric Ring Laser

In an effort to reduce arcing and yet raise energies, the anode mesh was replaced by 100, 5-mm wide rings spaced 5 mm apart, as shown in Fig. 4b. The current to each such ring was limited by a 1 kΩ resistor, similar to what was used in the pin-rod and pin-plate oscillators. CO_2:N_2:He - 1:1:3 gas mixtures at one-half an atmosphere of pressure again gave optimum results, and the capacitance could be doubled over that used in the Mesh

Laser. However, powers were not observed to increase appreciably.

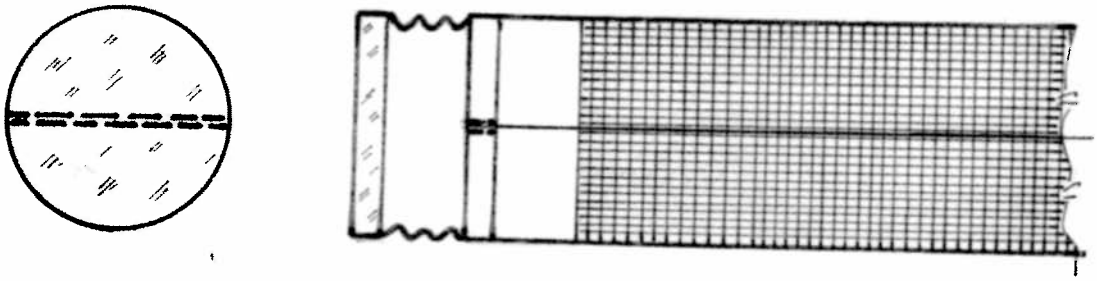

a) Mesh Laser

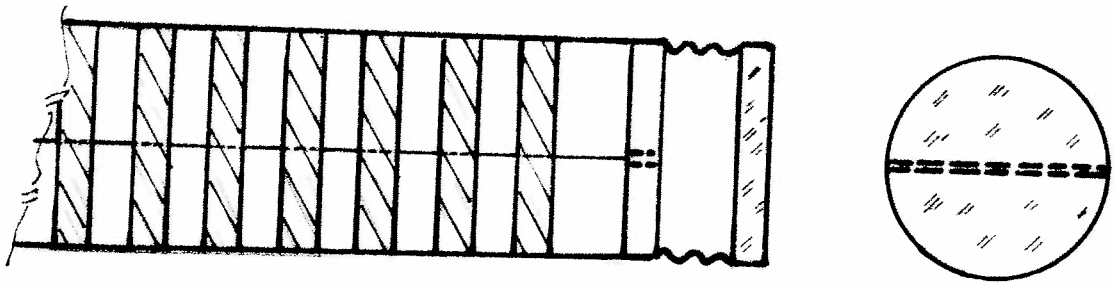

b) Ring Laser

Fig. 4 Concentric Electrode Lasers

The mode patterns of these concentric lasers were seen to be circularly symmetric rings, such as are usually associated with non-perturbed cylindrical cavities[20]. The lasing output, however, is not uniform across the area of the oscillator, and the distribution of such power was observed to vary from shot to shot.

IV. Discussion

A. Optimizing Electronic Excitation

It is not the purpose of this report to discuss the details of either the gaseous interaction processes within the oscillator, or the structure asso-

ciated with all potential longitudinal and transverse modes. A detailed treatment of the former can be found in the work of Patel[21], while the latter is discussed in some mathematical detail in the book by Sinclair and Bell[13]. However, some remarks are necessary concerning phenomena inherent in pulsed, high-power, transversely excited CO_2 lasers.

Of primary importance, during the electric discharge in the gas, is the prevention of strong arc formation within the laser cavity. Such arcs concentrate most of the electrical energy at a few discreet points in the oscillator, thereby preventing lasing action by impeding spatially homogeneous excitation throughout the gas volume. Arcing occurs when the jitter times between ignition of various points along the electrodes are large enough to be comparable to the time required for arc formation. In order to increase the time of the latter one can limit either the total capacitance of the energy source[14,22], or the individual capacitances, by placing separate capacitors at each discharge point[23], or one can limit the current by attaching a high-value resistor to each such point[11] (as has been done with the pin and ring lasers described herein). Alternatively, the jitter time can be reduced by employing Rogowski-profile contoured electrodes with various "third-electrode" preionization techniques[10,24-26], which appear to produce an adequate supply of "initial" electrons, via either photoelectric emission at the cathode surface or direct photoionization of the gas within the cavity by presumably the He $2^1P - 1^1S$ 584 Å resonance line. Although electrically more complex, such preionization schemes can produce greater population inversions by feeding energy into the gas more quickly prior to the commencement of lasing in free-running, or gain-switched, operation.

Once proper non-arcing, glow discharge conditions have been established the dominant process is the production of sufficiently energetic secondary electrons, by electron-molecule collisions of the primary electrons formed via positive-ion bombardment and photoelectric emission at the cathode .

These secondary electrons have the dual function of maintaining the discharge, as well as vibrationally exciting, either directly or indirectly, the CO_2 molecules. Theoretical analyses[27], for a CO_2:N_2:He - 1:1:8 gas mixture, suggest that optimum conditions exist for a ratio of electric field intensity to total neutral particle density $E/N \sim 3(10^{-16})$ V cm^2, where equal partition of energy occurs between the discharge-sustaining electron production and the lasing excitation.

B. Particle Interactions

Although direct vibrational excitation of the CO_2 by these secondary electrons is possible, most researchers have found stronger lasing for the more effective two-step interaction mechanism, whereby substantial numbers of N_2 molecules are raised to their metastable first vibrational level via collisions with secondary electrons, and subsequently transfer their energy by near-resonant encounters to the CO_2. This triatomic molecule is thereby raised into its asymmetric-stretch mode's first vibrationally excited level, from which lasing occurs:

a) $e + N_2(0) \longrightarrow e + N_2^*(1)$

b) $N_2^*(1) + CO_2(00^0 0) \longrightarrow N_2(0) + CO_2^*(00^0 1)$

c) $CO_2^*(00^0 1) \longrightarrow CO_2^*(10^0 0) + h\nu(10.6\ \mu)$

Addition of N_2 has been found, for certain conditions, to produce several lasing peaks during any one discharge. These secondary maxima can be mathematically predicted[28], and are physically due to the finite time required to transfer energy from the N_2 to the CO_2 during lasing action. In some interferometric diagnosis of transient plasma discharges, where the temporal isolation of a single event is necessary, such additional maxima are unwelcome, and lower power CO_2:He gas mixtures are usually used. It must be

noted that such secondary peaks were not evident in the study reported herein, possibly due to N_2 concentrations sufficiently small to allow all of the energy to be transferred to the CO_2 before the main laser pulse had terminated.

C. Gain Measurements

A number of researchers have also reported a high-frequency oscillation superimposed on the emitted radiation profile, suggesting a mode coupling, or "beat" interaction. The present observations have not confirmed this effect, possibly due to the relatively slow response times of the oscilloscopes. Such electronic limitations probably also account for the measured lower laser gains, with respect to those reported in the literature (4.3 - 5 % cm^{-1} [10]). Normally, when low power CW CO_2 lasers are available ultra-high response times are unnecessary, gains being measured by converting the oscillator into an amplifier. Under present conditions such gains were estimated from the leading edge of the radiation profiles emitted by the oscillator. Following Lengyel[29], and assuming losses due only to the mirrors at the ends of the cavity, an expression can be derived for the snall signal gain coefficient g in terms of the elapsed time t between two measurements of the laser intensity I_a and I_b, the speed of light c, the length of excited gas L, and the mirror reflectivities r_1 and r_2.

$$g = \ln \frac{(I_b/I_a)^{\frac{1}{ct}}}{(r_1 r_2)^{\frac{1}{2L}}} \qquad (9)$$

The response limitations of the electronics gave a lower bound on g approximating 0.6 % cm^{-1}, i.e., 7 to 8 times smaller than reported in ref. 10. Because extremely short response times of the order of 0.5 ns are required for precise measurements, it seems that amplifiers will be required to accurately determine gains.

Since g is proportional to the degree of population inversion, equ (9) suggests that maximum powers result when a given amount of electrical energy is fed into as small a volume of gas as possible, rather than distributing it over a larger domain. Such effects may partially explain the reduced power emitted by the larger excited volumes of the concentric lasers with respect to the pin configurations.

D. Radiation and Electric Field Effects

Optimum-gas-mixture emitted power versus applied voltage curves are shown in Fig. 5. Note that at 60 kV, for a 4-cm electrode gap operated at an atmospheric CO_2:N_2:He - 1.5:1.5:7 gas mixture, the power may not yet be maximum even though E/N ~ $6(10^{-16})$ V cm^2.

It is interesting to observe that whereas in an idealized linear electric discharge (in a rough sense applicable to all previously constructed transversely excited cavities) E is only a function of time, so that an optimum E/N should exist for the entire lasing volume at a given instant, E in a circularly symmetric discharge (concentric electrode lasers) is dependent on both radial position and time, thereby shifting the spatial location of optimum E/N conditions throughout the discharge time. The "fine-tuning" of discharge conditions for such lasers may, therefore, be simplified.

All of the lasing systems investigated so far have had similar pulse characteristics; for optimum gas mixtures and applied voltages pulses of less than 100 ns rise times and 60-150 ns half-widths occurred near the end of the electric discharge. Therefore, it is doubtful whether much power can be gained by Q-switching such cavities, for example by secondary gas absorption techniques[30,31].

V. Conclusions

A. The Pin Laser

A resistance-limited, 1.2-m long (1-m active volume), pin-plate, plane-parallel oscillator with output transmission of 50 % produced maximum powers of 20 MW. In this configuration pins were spaced 1 cm apart, with a 4-cm electrode gap, a system capacitance of 12 nF, and a maximum discharge voltage of 60 kV. Optimum lasing occurred for a CO_2:N_2:He - 1.5:1.5:7 gas mixture at atmospheric pressure. Emitted energies, calculated from the integration of radiation profiles, indicated maximum outputs of 2J, with associated electrical-to-radiation efficiencies approximating 9 %. Increasing the electrode separation to 6 cm, raising the capacitance to 24 nF, and changing the gas pressure and composition to a 0.4 — atmosphere 1:1:2 mixture, in order to prevent arcing, apparently doubled the output energy.

The plane-parallel cavity was found to be mechanically unstable, having to be continually adjusted for optimum lasing. Point focussing of the emitted radiation was good and caused air breakdown, by either direct or dust-particle stimulated means. Beam divergence was less than 5 milliradians. In contrast, a long-radius oscillator, employing a 5-m radius spherical mirror, was found to be mechanically very stable, with good shot-to-shot reproducibility of maximum powers, radiation delays, and pulse shapes , but with only one-half the maximum powers of the plane-parallel cavity.

For voltages near 60 kV electrical discharge times were approximately 1 μs in duration with maximum currents of about 18 A per pin. Under optimum gas mixtures, pressures, and applied voltage conditions the onset of lasing occurred near the end of the discharge, and had a pulse half-width of 60-150 ns. Linear and circularly-symmetric higher order mode patterns were seen. The high degree of external focussing obtainable with the plane - parallel configuration suggest that for this cavity the greater part of the

energy is carried in the lowest order mode, whose beam divergence is very small.

B. Concentric Electrode Lasers

Concentric electrode configurations, employing a central wire cathode and a surrounding mesh or ring anode, lased in both the long-radius and plane-parallel configurations, but at reduced power levels maximizing at approximately 1.4 MW. Although visual observations indicated relatively uniform discharge conditions throughout the lasing volume, the circularly-symmetric mode output patterns showed random intensity fluctuations across the beam. Empirical data indicate that cavity perturbations, caused by the cathode wire and strut assembly, would not account for these relatively low powers. Additional analyses are required to explain such results.

Acknowledgement

The author expresses his gratitude to K. Hruska for his excellent designs, H. Ripper for making the optical components and the gas handling system, J.-L. Martin and his personnel for constructing the various lasers, E. Striberni for installing the electrical system, and J. Bovey for patiently typing the sometimes hard-to-read manuscript.

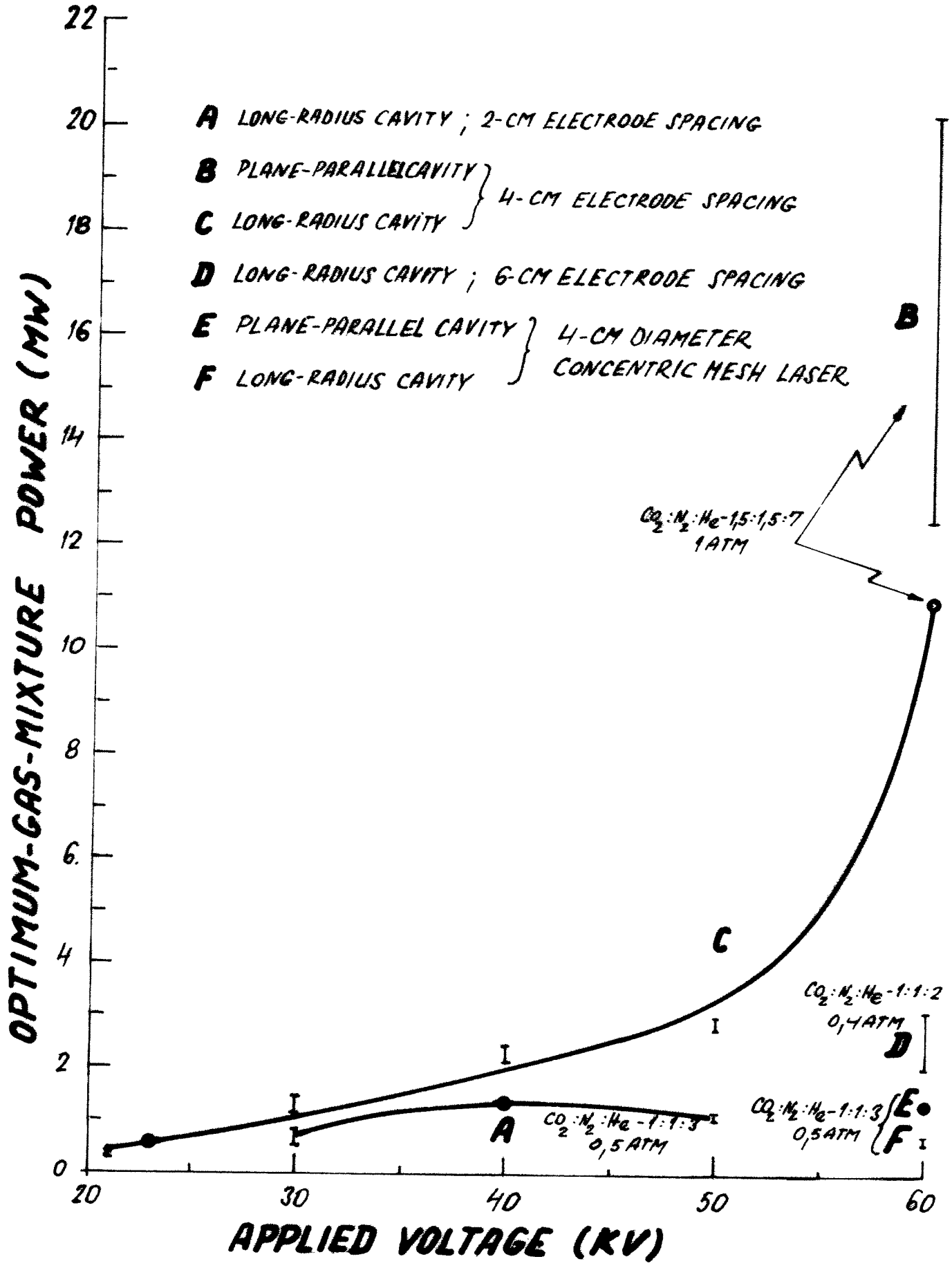

Fig. 5 Laser Emission at Optimum Gas Mixtures and Pressures (C = 12 nF)

References

1. H.R. Griem, Plasma Spectroscopy (McGraw-Hill Book Co., New York, 1964) pp 267-313

2. S. Kobayashi and K. Kurihara, Appl. Phys. Lett. 19, 482 (1971)

3. P.R. Forman, F.C. Jahoda, and R.W. Peterson, Appl. Opt. 11, 477 (1972)

4. G. Decker, H. Herold, and H. Röhr, Appl. Phys. Lett. 20, 490 (1972)

5. D.E. Evans and J. Katzenstein, Rep. Prog. Phys. 32, 207 (1969)

6. A. Unsöld, Physik Der Sternatmosphären (Springer-Verlag, Berlin, 1955) p 294

7. I.K. Pasco, Masters Thesis, Culham Laboratory (1968)

8. J.M. Dawson, R.E. Kidder, and A. Hertzberg ,Princeton University MATT-782 (1971)

9. K. Brueckner, Physics Today (Search and Discovery) Aug. 1972

10. M.C. Richardson, A.J. Alcock, K. Leopold, and P. Burtyn, Proc. of Symposium on High Power Molecular Lasers, Laval University, Quebec, May 15-17, 1972

11. A.J. Beaulieu, Appl. Phys. Lett. 16, 504 (1970)

12. A.L. Bloom, Gas Lasers (John Wiley and Sons, New York, 1968) p 74

13. D.C. Sinclair and W.E. Bell, Gas Laser Technology (Holt Rinehart and Winston, Inc., New York, 1969) p 8

14. K.A. Laurie and M.M. Hale, IEEE J. Quant. Electr. QE-7, 530 (1971)

15. E.S. Weibel, LRP 50/71, CRPP, Lausanne (1971)

16. J.D. Cobine, Gaseous Conductors (Dover Publications, Inc., New York, 1958) p 250

17. R.J. Carbine and W.J. Witteman, IEEE J. Quant. Electr. QE-5, 442 (1969)

18. A. Därr, G. Decker, and H. Röhr, Z. Physik 248, 121 (1971)

19. M.A. Bramson, Infrared Radiation: A Handbook for Engineers (Plenum Press, New York, 1968) p 582

20. D. Röss, Lasers: Light Amplifiers and Oscillators (Academic Press, London, 1969) p 176

21. C.K.N. Patel, Gas Lasers (in Lasers, Vol. 2, ed. by A.K. Levine, Marcel Dekker, Inc., New York, 1968)

22. K.A. Laurie and M.M. Hale, IEEE J. Quant. Electr. QE-6, 530 (1970)

23. D.C. Johnson, IEEE J. Quant. Electr. QE-7, 185 (1971)

24. A.K. Laflamme, Rev. Sci. Instr. 41, 1578 (1970)

25. P.R. Pearson and H.M. Lamberton, IEEE J. Quant. Electr. QE-8, 145 (1972)

26. R. Dumanchin et al, IEEE J. Quant. Electr. QE-8, 163 (1972)

27. W.L. Nighan and J.H. Bennett, Appl. Phys. Lett. 14, 240 (1969)

28. G.C. Vlases and W.M. Moeny, J. Appl. Phys. 43, 1840 (1972)

29. B.A. Lengyel, Lasers (John Wiley and Sons, Inc., New York, 1962) p 32

30. T.Y. Chang, C.H. Wang, P.N. Cheo, Appl. Phys. Lett. 15, 157 (1969)

31. R.E. Jensen and M.S. Tobin, IEEE J. Quant. Electr. QE-6, 477 (1970)